Journal of the Ceramic Society of Japan 130 [1] 81-87 2022
DOI http://doi.org/10.2109/jcersj2.21119

JCS-Japan

FULL PAPER

Evaluation of calcium phosphate coating on biodegradable Mg–Al–Zn–Ca alloy formed under ordinary conditions on temperature and pressure

Kenshiro TAKAISHI[1], Shigeomi TAKAI[1] and Takeshi YABUTSUKA[1,†]

[1] Department of Fundamental Energy Science, Graduate School of Energy Science, Kyoto University, Yoshida-honmachi, Sakyo-ku, Kyoto 606–8501, Japan

Octacalcium phosphate (OCP) coating was formed on the surface of Mg–Al–Zn–Ca alloy (AZX612) by anodically oxidized and subsequently immersed in a supersaturated aqueous solution containing phosphate and calcium ion under ordinary temperature and pressure. The formed OCP layer consisted of both the inner layer of the fine crystallites and the outer layer of the large crystallites, and the inner layer remained on the alloy even after the ultrasonication process. In simulated body fluid, AZX612 treated with both anodic oxidization and subsequent OCP coating process showed higher corrosion resistance than those treated with only anodic oxidization.

Key-words : Phosphate salt, Calcium phosphate coating, Magnesium alloy, Ordinary temperature and pressure process, Corrosion resistance

[Received July 18, 2021; Accepted October 19, 2021]

1. Introduction

In today's superaged society, demand for novel implant materials with high bone-bonding ability has increased. Among them, bioabsorbable implant materials have been widely in clinical use because these materials have attractive points to replace new bone gradually and spontaneously. Bioabsorbable ceramics such as β-tricalcium phosphate are one of the most attractive implant materials with both good bone-bonding ability and bio-absorbability. However, ceramic materials are generally brittle and sensitive to impact in comparison with metallic or polymeric ones. Bioabsorbable polymers such as polylactic acid are also widely used in orthopedic surgery. However, conventional bioabsorbable polymers generally showed lower mechanical strength than human cortical bone. Hence, bioabsorbable or biodegradable implant materials with suitable mechanical properties, suitable replaceability with newly formed bone, and good bone-bonding ability have been required in clinical fields.

Recently, magnesium (Mg) and its alloys have been researched as a new candidate as biodegradable implant material. Mg is a bio-essential element, and approximately 25 g of Mg is initially contained in the living human body.[1] Therefore, Mg and its alloys are expected to be useful for biodegradable metallic implant materials with both mechanical toughness and bio-absorbability. However, it is well known that conventional Mg alloys are decomposed in a short time in the living body. When Mg is dissolved from Mg and its alloys in the living body, it releases hydrogen gas according to Eqs. (1)–(3).[2]

$$Mg \rightarrow Mg^{2+} + 2e^- \quad (1)$$

$$2H_2O + 2e^- \rightarrow H_2 + 2OH^- \quad (2)$$

$$Mg^{2+} + 2OH^- \rightarrow Mg(OH)_2 \quad (3)$$

If the Mg alloy is used as an implant material without surface treatment, it has been reported that a space derived from generated hydrogen gas was formed between the alloy and the tissue.[3),4)] Hence, it is essential to control the degradation rate of the alloys by improving the corrosion resistance in order to use them as bone fixation in clinical use.

In order to improve the corrosion resistance of Mg alloys, several types of surface modification techniques have been proposed to form a stable coating on the Mg alloy surface. For example, Mg inorganic compounds such as MgO,[5)] MgF_2,[6)] TiO_2,[7)] and bioabsorbable polymers such as polylactic acid, polycaprolactam,[8)] and chitosan[9)] are proposed as coating materials on the Mg alloys to control Mg degradation. Among them, calcium phosphate is one of the most effective coating materials because of its biocompatibility and osteoconductivity. It has been reported that the formation of calcium phosphate such as hydroxyapatite on Mg alloys progressed according to Eqs. (1), (2), and (4).[10)]

† Corresponding author: T. Yabutsuka; E-mail: yabutsuka@energy.kyoto-u.ac.jp
‡ Preface for this article: DOI http://doi.org/10.2109/jcersj2.130.P1-1

$$(10-x)Ca^{2+} + xMg^{2+} + 6PO_4^{3-} + 2OH^- \rightarrow Ca_{10-x}Mg_x(PO_4)_6(OH)_2 \quad (4)$$

Octacalcium phosphate (OCP) is a precursor of hydroxyapatite, which is the main component of human bones. It has been reported that the OCP has both suitable stability and bio-absorbability in the living body.[11] The latter point, in particular, is one of the characteristics of OCP that hydroxyapatite does not show. If the coating methodology of OCP on Mg alloys is established, this will be a promising technique to improve the degradation property and osteoconductivity of the Mg alloys because the coating material, OCP, shows the above two properties.

It has been reported that calcium phosphates could be coated on Mg alloys surface by electrodeposition,[12] electrophoretic deposition,[13] high-temperature aqueous solution synthesis,[14] a sol–gel method,[15] etc. Among them, the aqueous solution method is a method of forming a coating on the surface of a substrate by immersing the substrate in an aqueous solution under ordinary temperature and pressure conditions, and does not require special equipment, high temperature, and high pressure and can be carried out at a low cost. However, it takes a long time to form the coating and generally needs a high-temperature environment to promote calcium phosphate formation. If the calcium phosphate coating techniques under ordinary temperature are developed, therefore, this is an advantageous method to apply various types of unstable substrates such as pure Mg. In the previous study, we proposed the formation process of OCP coating on the Mg–3Al–1Zn alloy (AZ31) surface by anodic oxidization and subsequent formation of OCP coatings in an aqueous solution under ordinary temperature and pressure and reported its corrosion behavior of the OCP-coated AZ31 in biomimetic solution.[16]

Calcium is relatively less toxic in comparison with many types of metallic components, and it has been reported that calcium was easily incorporated into the living bones when it co-existed with Mg.[17] Based upon this knowledge, Mg alloys containing calcium will be expected to improve bone repairing. In this study, we aimed to develop a preparation process of OCP coating on the Mg–6Al–1Zn–2Ca alloy (AZX612), which is the Mg alloy containing calcium, in an aqueous solution under ordinary temperature and pressure and clarify the effect of the OCP coating on corrosion behavior of the AZX612 in biomimetic solution.

2. Materials and methods

The surface of the AZX612 specimen (Standard Test Piece, Japan) was polished using #1200 SiC abrasion paper, washed with acetone, ethanol, and distilled water in an ultrasonic cleaner, and air-dried.

The anodic oxidization of the surfaces of the specimens was carried out in a 1 mol·dm^{-3} NaOH aqueous solution by applying 10 V of constant voltage for 10 min. The surfaces of the specimens were washed in distilled water and air-dried.

The aqueous solution containing 7.5 mmol·dm^{-3} Ca^{2+}, 3.0 mmol·dm^{-3} HPO_4^{2-}, 6.0 mmol·dm^{-3} K^+ and 15.0 mmol·dm^{-3} Cl^- was prepared by dissolving reagent grade $K_2HPO_4 \cdot 3H_2O$ (Nacalai Tesque, Japan) and $CaCl_2$ (Fujifilm Wako) in distilled water, and this solution was adjusted at pH = 6.00, 36.5 °C by dissolving 1 mol·dm^{-3} HCl and $(CH_2OH)_3CNH_2$ (Fujifilm Wako). This solution is denoted as 'CaP solution,' hereafter. After polishing or subsequently anodic oxidizing, the specimen was immersed in 50 dm^3 in CaP solution for 2 or 12 h to form a calcium phosphate coating on the AZX612. Ultrasonication was carried out on the specimen in acetone for 10 min for removing fragile calcium phosphate pieces from the specimens.

The surface and the cross-section of the specimen was evaluated by scanning electron microscope (SEM, SU6600, Hitachi High-Technologies, Japan), energy dispersive X-ray analyzer (EDX, XFlash® 5010, Bruker, USA), thin-film X-ray diffraction (XRD, RINT 2500, Rigaku, Japan) using Cu Kα radiation at 50 kV and 50 mA of tube voltage and current, or X-ray photoelectron spectroscopy (XPS, JPS-9030, JEOL, Japan) using Mg Kα radiation at 12 kV and 50 mA of acceleration voltage and emission current.

Thus-treated AZX612 was immersed in simulated body fluid (SBF) at 36.5 °C for 20 days, and the dissolution of Mg, that is, decomposition of the alloy, was evaluated by measuring the volume of generated hydrogen gas. The effects of the anodic oxidization treatment and the CaP solution treatment on the generated amount of hydrogen gas were investigated.

3. Result and discussion

Figure 1 shows the XRD and XPS results of the surface of the AZX612 before and after the anodic oxidization. Refering to the reports by Serizawa et al.[18] and Yuasa et al.,[19] peaks of Mg, Al_2Ca, $Mg_{17}Al_{12}$, and Al–Mn compounds were observed in the both XRD patterns. It is considered that the unmarked peaks, which were not observed in the above references, were derived from some compounds generated by the manufacturing process of the untreated substrate. In the XRD results of the anodically oxidized AZX612, broad peaks of MgO were slightly detected. This result suggested that the precipitated oxides were amorphous phase or their amount was tiny even if they were crystal phase. In the XPS results, on the other hand, the peak of Mg2p shifted to higher binding energy after the anodic oxidization. These results suggested that a small amount of MgO or its amorphous phase was formed on the surface of the AZX612 by the anodic oxidization process.

Figure 2 shows the XRD patterns of the surface of AZX612 immersed in CaP solution for 0, 2, or 12 h without anodically oxidizing. The sharp diffraction peaks were detected at 4.7° after immersion in the CaP solution for 2 h. This peak was the main peak of OCP. The intensity and number of peaks attributed to OCP increased after immersion in CaP solution for 12 h. This result indicated

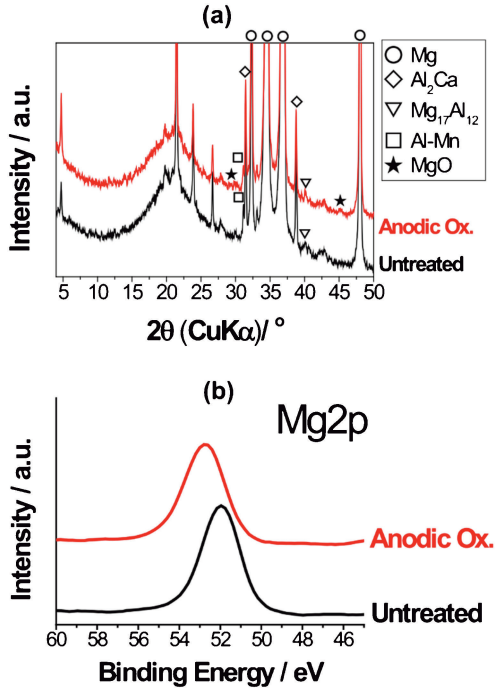

Fig. 1. Results of (a) XRD and (b) XPS of the surface of the AZX612 before and after the anodic oxidization.

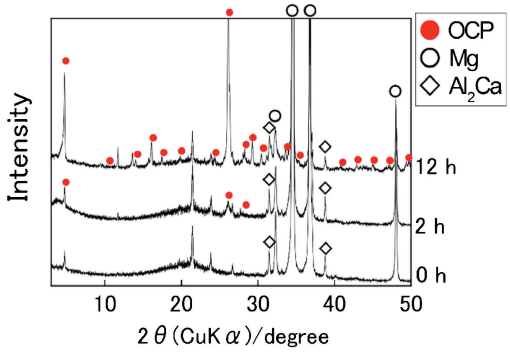

Fig. 2. XRD patterns of the surface of AZX612 immersed in CaP solution for 0, 2, or 12 h.

that the AZX612 possessed OCP formation ability in the CaP solution. In contrast, it can be seen that the OCP formed within 2 h was not transformed to hydroxyapatite because the peak at 4.7° was further intensified after 12 h. It is speculated that the existence of Mg might prohibit the crystallization of OCP to hydroxyapatite.

Figure 3 shows the XRD patterns of the surface of AZX612 anodically oxidized and subsequently immersed in CaP solution for 0, 2, or 12 h. Similar to the results without anodic oxidization shown in Fig. 1, the sharp diffraction peaks of OCP were detected at 4.7° after immersion in the CaP solution for 2 h. In addition, the intensity and number of peaks attributed to OCP increased after immersion in CaP solution for 12 h, similar to the case without anodic oxidization.

Figure 4 shows the SEM images of the surface of AZX612 immersed in CaP solution and those anodically oxidized and subsequently immersed in CaP solution.

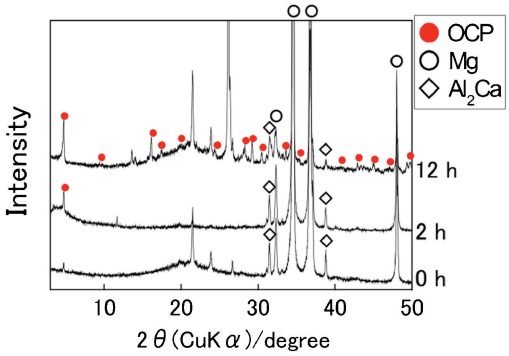

Fig. 3. XRD patterns of the surface of AZX612 treated with polishing, anodizing, and subsequent immersing in CaP solution for 0, 2, or 12 h.

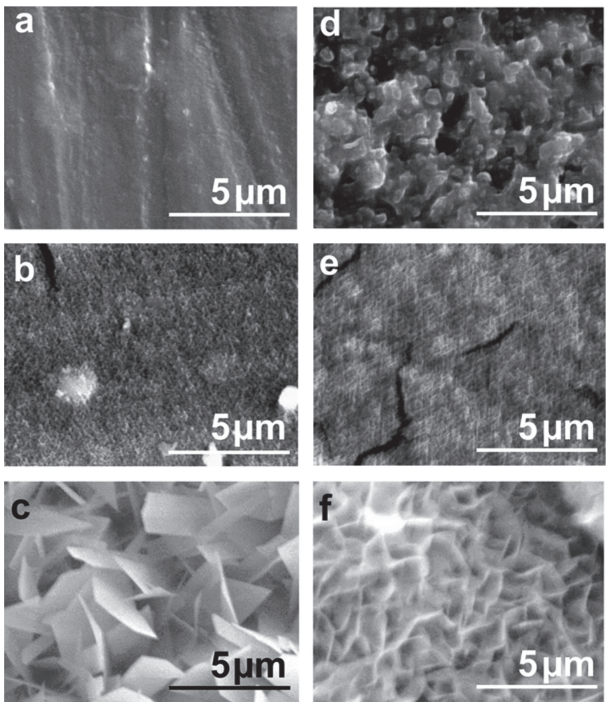

Fig. 4. SEM images of (a–c) the surface of AZX612 immersed in CaP solution for (a) 0, (b) 2 or (c) 12 h, and (d–f) those anodically oxidized and subsequently immersed in CaP solution for (d) 0, (e) 2 and (f) 12 h.

After the anodic oxidization, some precipitates were newly formed on the whole surface of the specimen, as shown in Fig. 4(b). It is considered that the observed precipitates were oxide film formed by the anodic oxidization. After the immersion in CaP solution for 2 h, fine flake-like crystallites were formed on the whole surface of the specimens regardless of the anodic oxidization, as shown in Figs. 4(b) and 4(e). Taking into consideration the results of the XRD, the flake-like crystallites were considered to consist of OCP as the main component. After the immersion for 12 h, the size of the crystallites became bigger than that for 2 h, and plate-like crystallites were formed, as shown in Figs. 4(c) and 4(f). The size of the plate-like crystallites in the case of without anodic oxidization was larger than that with anodic oxidization. Taking into con-

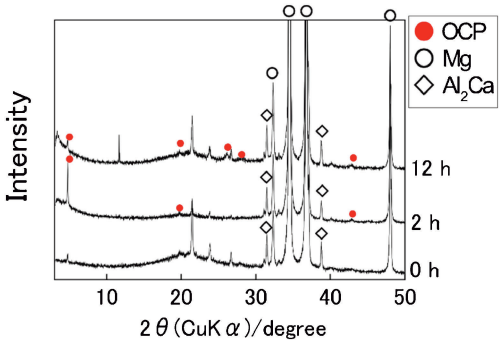

Fig. 5. XRD patterns of AZX612 immersed in the CaP solution for 0, 2, and 12 h and then treated with ultrasonication in acetone.

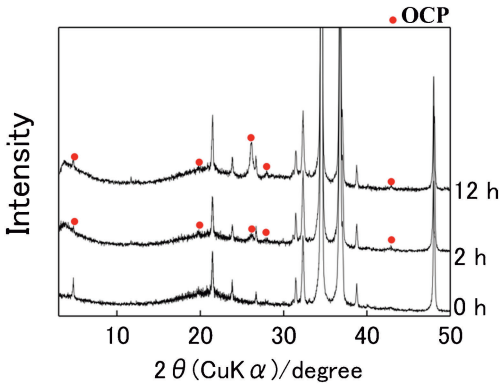

Fig. 6. XRD patterns of AZX612 anodically oxidized, immersed in the CaP solution for 0, 2, and 12 h, and then treated with ultrasonication in acetone.

sideration the results of the XRD, the precipitates formed by the immersion for 12 h were considered to consist of OCP as the main component, too. Especially in the case of without anodic oxidization, however, the precipitates formed on the surface after 12 h immersion looked to be fragile. From the results shown in Figs. 2–4, it is suggested that the OCP crystallites were formed on the specimens by immersing in the CaP solution regardless of the anodic oxidization, and then their morphologies were changed from fine flake crystallites to relatively larger size plate-like ones as the immersion time increased.

Figure 5 shows the XRD patterns of the AZX612 immersed in the CaP solution and then treated with ultrasonication in acetone. The obtained XRD pattern in the case of the immersion for 2 h was almost similar to that before ultrasonication shown in Fig. 2. In the case of the immersion for 12 h, however, the number and intensity of diffraction peaks attributed to OCP decreased in comparison with before ultrasonication shown in Fig. 2. It was considered that the fragile OCP crystallites shown in Fig. 4(c) were removed by the ultrasonication process, and the amount of the remaining OCP on the specimen was reduced.

Figure 6 shows the XRD patterns of the AZX612 anodically oxidized, immersed in the CaP solution, and then treated with ultrasonication in acetone. In the case of the immersion for 12 h, similar to the case of that without

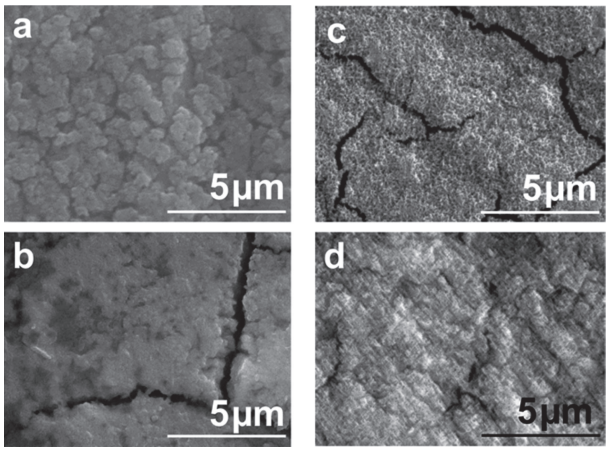

Fig. 7. SEM images of (a, b) the surface of the AZX612 immersed in the CaP solution for (a) 2 or (b) 12 h and then treated with ultrasonication, and (c, d) those anodically oxidized, immersed in the CaP solution for (c) 2 and (d) 12 h, and then treated with ultrasonication.

anodic oxidization, the number and intensity of diffraction peaks attributed to OCP decreased in comparison with before ultrasonication shown in Fig. 3. It was considered that the amount of the remained OCP on the specimen was reduced, similar to the case without anodic oxidization.

Figure 7 shows the SEM images of the surface of thus OCP-coated AZX612 treated with ultrasonication. For all the types of specimens, fine crystallites were observed on the whole surface regardless of the anodic oxidization and immersion time in the CaP solution. In the case of the immersion for 12 h, in particular, it can be seen that the plate-like crystallites which had been observed before ultrasonication was not observed. Taking into consideration the results of the XRD and SEM, it was considered that ultrasonication removed the larger size of plate-like OCP crystallites and remained the fine crystallites on the surface of the AZX612 immersed for 12 h, although those immersed for 2 h did not show considerable difference in the surface morphology in comparison with those for 12 h.

Figure 8 shows the SEM images and EDX line-scanning spectra of the cross-section of AZX612 immersed in the CaP solution, and those anodically oxidized and then immersed in the CaP solution. For the specimens immersed for 2 h, it can be seen that coating containing calcium and phosphorus as its components, that is, OCP coating, with ca. 2 μm in thickness, was formed on the specimen regardless of the anodic oxidization. For the specimens immersed for 12 h, in contrast, it can be seen that the OCP coating with ca. 6–7 μm in thickness was formed on the specimen regardless of the anodic oxidization. From these results, it was found that the OCP coating grew and increased in thickness as the immersion time in CaP solution increased. Taking into consideration the SEM and EDX results, in addition, it can be seen that boundary was observed inside the OCP coatings for the specimens immersed for 12 h regardless of the anodic oxidization. Such boundary was not observed for the 2 h specimens. Hence, it is considered that the OCP coating on the 2 h

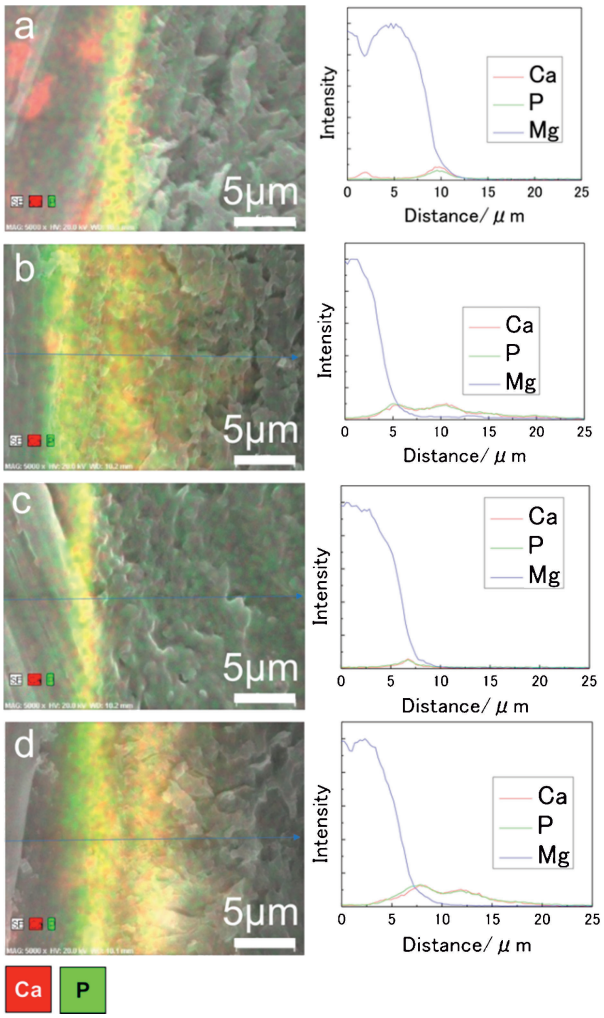

Fig. 8. SEM images and EDX line-scanning spectra of the cross-section of (a, b) AZX612 immersed in the CaP solution for (a) 2 or (b) 12 h, and (c, d) those anodically oxidized and then immersed in the CaP solution for (c) 2 or (d) 12 h.

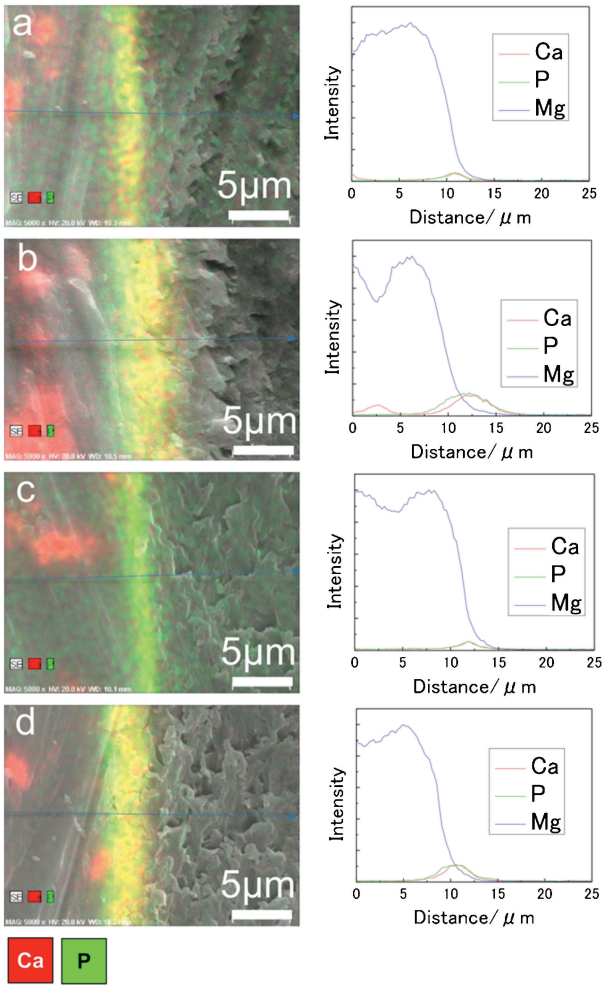

Fig. 9. SEM images and EDX line-scanning spectra of the cross-section of (a, b) AZX612 immersed in the CaP solution for (a) 2 or (b) 12 h and then treated with ultrasonication, and (c, d) those anodically oxidized, immersed in the CaP solution for (c) 2 or (d) 12 h, and then treated with ultrasonication.

specimens consisted of a single layer with fine OCP crystallites and that 12 h double layers with an inner one of fine OCP and an outer one of large OCP.

Figure 9 shows the SEM images and EDX line-scanning spectra of the cross-section of AZX612 immersed in the CaP solution and then treated with ultrasonication, and those anodically oxidized, immersed in the CaP solution, and then treated with ultrasonication. For the specimens immersed for 2 h, it can be seen that the thickness of the OCP coating was not so changed even after the ultrasonication regardless of the anodic oxidization. This result indicates that the OCP coating was hardly removed by ultrasonication. For the specimens immersed for 12 h, in contrast, it can be seen that the thickness of the OCP coating was reduced after the ultrasonication regardless of the anodic oxidization and almost corresponded to that of the inner layer shown in Figs. 8(b) and 8(d). From the results shown in Figs. 4 and 6–8, it is considered that the double-layered OCP coating was formed by the immersion of AZX612 for 12 h, and then the fragile outer OCP layer was almost removed by the ultrasonication process, and the inner layer of the fine OCP crystallites almost remained even after the ultrasonication. Such results were quite similar to the case of AZ31, which we reported previously.[16] Hence, this phenomenon was most likely dominated by the behavior of magnesium, the main component of the Mg alloys.

The formation mechanism of the OCP coating on AZX612 is considered as follows. In the early stage of the AZX612 immersion in the CaP solution, the pH and Mg ion concentration locally increased near the surface of AZX612 according to Eqs. (1) and (2). Then, the local increase in the pH promoted nucleation and formation of calcium phosphate, according to Eq. (4). Because the pH of the CaP solution was buffered at 6.00, 36.5 °C in this study, the formed calcium phosphate was crystallized as OCP instead of hydroxyapatite. It has been reported that the existence of Mg ions inhibits calcium phosphate crystallization.[20] In this stage, however, the size of the OCP crystallites was not so large because Mg ions slightly released from AZX612 inhibited crystal growth of the OCP. In fact, it has been reported that the growth of OCP crystals was

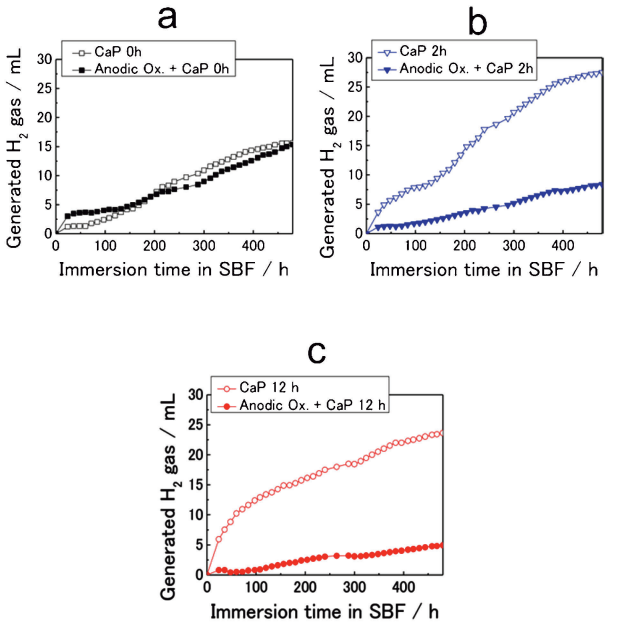

Fig. 10. Changes in volume of hydrogen gas released from SBF in which AZX612 coated with OCP by the immersion in the CaP solution for (a) 0, (b) 2, or (c) 12 h was immersed. In each graph, the results both with and without anodic oxidization before the CaP solution treatment are shown.

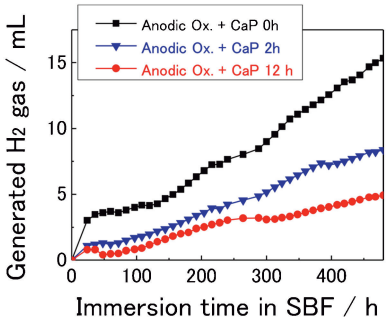

Fig. 11. Comparison of the changes in the volume of generated hydrogen gas released from SBF when AZX612, which were anodically oxidized and subsequently immersed in the CaP solution for 0, 2, or 12 h, were immersed in SBF.

suppressed in the presence of Mg ions because Mg, which has a smaller ionic size than Ca, replaced Ca in OCP.[21] Once the fine OCP formed coating on the surface of AZX612, the release of Mg ion from the AZX612 was suppressed, and the large OCP crystallites grew on the fine OCP layer. In this OCP formation stage, the OCP crystallites tended to grow vertically against the substrate by the geometrical selection of crystal growth direction because the crystals grown parallel to the substrate could not grow further because of the collides with each other.

In this study, the formed OCP coatings in the case of AZX612 treated with both anodic oxidization and the CaP solution for 12 h showed ca. 6–7 µm in thickness and ca. 3 µm even after the ultrasonication. It has been reported that hydroxyapatite coatings with 6.3 µm in average thickness had been prepared by the sol–gel method.[15] Although the thicknesses of the coatings were comparative level, the sol–gel method took more than 48 h from immersion in a solution containing calcium and phosphate to completion of the coating and requires heating to a maximum of 60 °C. The advantage of the OCP coating in this study is considered to be a shorter coating time and an ordinary reaction temperature. Hence this method has the possibility to apply to more unstable and reactive substrates.

Figure 10 shows the changes in the volume of hydrogen gas released from SBF in which AZX612 is coated with OCP. In Fig. 10, the difference in hydrogen gas generation with and without anodic oxidization for each immersion time in the CaP solution. Without the CaP solution treatment, the volume of hydrogen gas released from AZX612 was almost similar in the case of with or without anodic oxidization throughout the SBF immersion time, as shown in Fig. 10(a). In the case of the OCP-coated AZX612, in contrast, the specimen treated with anodic oxidization before the CaP solution treatment showed a considerably lower volume of the generated hydrogen than those without anodic oxidization throughout the SBF immersion time. From the results shown in Fig. 10, it is considered that the combination of anodic oxidation and OCP coating is effective in improving the corrosion resistance of AZX612. It has been reported that immersion solution often penetrated into the calcium phosphate coating, and corrosion progressed on the interface between the calcium phosphate coating and the Mg alloy substrates.[22] In this study, the OCP coating was formed by immersing 99.8 % pure Mg substrates in an aqueous solution containing 0.25 mol·L^{-1} Ca-EDTA and KH_2PO_4 for 2 h.[23] However, the morphology of the OCP coating was similar to our study, with a two-layer structure consisting of a relatively dense inner layer and a coarse outer layer.

From these findings, it is considered that the anodic oxidization improved the corrosion resistance of AZX612 because the oxidized film acted as a role to protect AZX612 from SBF, which penetrates OCP coating.

Figure 11 shows the comparison of the changes in the volume of generated hydrogen gas released from SBF when AZX612, which were anodically oxidized and subsequently immersed in the CaP solution for 0, 2, or 12 h, were immersed in SBF. The volume of the generated hydrogen gas decreased with increasing immersion time in the CaP solution. In the case of the immersion in the CaP solution for 12 h, the volume of hydrogen gas was reduced by up to 70 % compared to without the CaP solution treatment. From the results shown in Fig. 11, it is considered that corrosion resistance improved as immersion time increased. It has been reported that the biomimetic method reduced the corrosion rate of Mg by ca. 40–90 %.[24] However, a part of the conventional methods requires heating above 60 °C. In this study, on the other hand, the comparative level of corrosion rate was achieved by immersion in the CaP solution at ordinary temperature by combining the anodic oxidization. This point is the advantageous point of this study; that is, the corrosion resistance could be improved to the comparative level as the conventional

methods under a soft environment which is advantageous for application for more unstable, reactive, and degradable Mg alloys.

4. Conclusion

The double-layered OCP coating on AZX612 was formed by the formation of flake-like crystallites and then the growth of plate-like crystallites by immersed in the CaP solution for 12 h under ordinary temperature and pressure. However, the plate-like crystallites in the outer layer were brittle and easily removed by the ultrasonication process, and the inner OCP layer with ca. 3 µm in thickness remained even after the ultrasonication. The OCP-coated AZX612 showed higher corrosion resistance than uncoated AZX612, and the volume of hydrogen gas generation in SBF was suppressed by up to 70 % in maximum. The anodic oxidization before the CaP solution treatment improved the corrosion resistance of AZX612. The OCP coating process proposed in this study will be expected as a novel surface modification technique to improve both corrosion behavior and the bone-bonding ability of Mg alloys in the living body.

References

1) J. Vormann, *Mol. Aspects Med.*, **24**, 27–37 (2003).
2) G. L. Song and A. Atrens, *Adv. Eng. Mater.*, **1**, 11–33 (1999).
3) D. Noviana, D. Paramitha, M. F. Ulum and H. Hermawan, *J. Orthop. Transl.*, **5**, 9–15 (2016).
4) F. Witte, V. Kaese, H. Haferkamp, E. Switzer, A. Meyer-Lindenberg, C. J. Wirth and H. Windhagen, *Biomaterials*, **26**, 3557–3563 (2005).
5) X. N. Gu, N. Li, W. R. Zhou, Y. F. Zheng, X. Zhao, Q. Z. Cai and L. Ruan, *Acta Biomater.*, **7**, 1880–1889 (2011).
6) K. Y. Chiu, M. H. Wong, F. T. Cheng and H. C. Man, *Surf. Coat. Tech.*, **202**, 590–598 (2007).
7) J. Hu, C. Zhang, B. Cui, K. Bai, S. Guan, L. Wang and S. Zhu, *Appl. Surf. Sci.*, **257**, 8772–8777 (2011).
8) L. Xu and A. Yamamoto, *Appl. Surf. Sci.*, **258**, 6353–6358 (2012).
9) B. D. Hahn, D. S. Park, J. J. Choi, J. Ryu, W. H. Yoon, J. H. Choi, H. E. Kim and S. G. Kim, *Surf. Coat. Tech.*, **205**, 3112–3118 (2011).
10) J. E. Gray-Munro and M. Strong, *J. Biomed. Mater. Res. A*, **90**, 339–350 (2009).
11) H. Uoda, E. Matsuda, T. Yamamoto and H. Mori, *J. Soc. Powder Technol., Jpn.*, **48**, 600–605 (2011).
12) C. Wen, S. Guan, L. Peng, C. Ren, X. Wang and Z. Hu, *Appl. Surf. Sci.*, **255**, 6433–6438 (2009).
13) R. M. Kumar, K. K. Kuntal, S. Singh, P. Gupta, B. Bhushan, P. Gophinath and D. Lahiri, *Surf. Coat. Tech.*, **287**, 82–92 (2016).
14) M. Tomozawa and S. Hiromoto, *Acta Mater.*, **59**, 355–363 (2011).
15) R. Rojaee, M. Fathi and K. Raeissi, *Mater. Sci. Eng., C*, **33**, 3817–3825 (2013).
16) S. Watanabe, T. Yabutsuka and S. Takai, *Key Eng. Mat.*, **782**, 158–164 (2018).
17) C. M. Serre, M. Papillard, P. Chavassieux, J. C. Voegel and G. Boivin, *J. Biomed. Mater. Res.*, **42**, 626–633 (1998).
18) A. Serizawa, Y. Iwase, T. Sudare, N. Saito, N. Kamiyama and T. Ishizaki, *J. Jpn. Inst. Light Met.*, **66**, 9–14 (2016).
19) M. Yuasa, E. Yukutake, X. Huang, K. Suzuki, N. Saito and Y. Chino, *J. Jpn. Inst. Light Met.*, **66**, 266–272 (2016).
20) A. Bigi, G. Falini, E. Foresti, A. Ripamonti, M. Gazzano and N. Roveri, *J. Inorg. Biochem.*, **49**, 69–78 (1993).
21) E. Boanini, M. Gazzano, K. Rubini and A. Bigi, *Cryst. Growth Des.*, **10**, 3612–3617 (2010).
22) S. Hiromoto, *J. Jpn. Inst. Light Met.*, **64**, 203–210 (2014).
23) M. Tomozawa and S. Hiromoto, *Acta Mater.*, **59**, 355–363 (2011).
24) F. Witte and A. Eliezer, in "Degradation of Implant Materials", Ed. by N. Eliaz, Springer, New York (2012) pp. 93–109.